Comparison of Left Function Assessment Using Phonocardiogram and Electrocardiogram Triggered 2D SSFP CINE MR Imaging at 1.5 T and 3.0 T

T. Frauenrath[1], M. Becker[2,3], F. Hezel[1], G. A. Krombach[2], U. Kremer[2], J. Schulz-Menger[1,3], and T. Niendorf[1,3]

[1]Berlin Ultrahigh Field Facility, Max-Delbrueck Center for Molecular Medicine, 13125 Berlin, Germany, [2]Department of Radiology, University Hospital, RWTH, 52074 Aachen, Germany, [3]Experimental and Clinical Research Center (ECRC), Charité Campus Buch, Humboldt-University, 13125 Berlin, Germany

Introduction:

In clinical MRI cardiac motion is commonly dealt with using ECG based synchronization. As high-field cardiac MRI becomes more widespread the propensity of ECG recordings to interference from electromagnetic fields (EMF) and to magneto-hydrodynamic (MHD) effects increases [1]. Consequently, artifacts in the ECG trace may result in mis-triggering causing motion corrupted image quality. Realizing these limitations a MR-stethoscope (ACT) has been proposed for a practical gating/triggering alternative which meets the demands of cardiac/triggered [2,3]. Motivated by the challenges of conventional ECG together with the advantages of acoustic cardiac gating, this study compares phonocardiogram and ECG triggered MRI to explore the suitability, efficacy and robustness of ACT for the assessment of LV function. For this purpose endocardial border sharpness (EBS) was examined through an objective measurement of acutance (4) paralleled by quantitative LV function assessment.

Methods:

A comparative volunteer study including healthy subjects (n=14) with no history of cardiovascular disease was performed on a 1.5 T and a 3.0 T MR system (Achieva, Philips, Best, The Netherlands). Conventional vector ECG (VCG) and acoustic trigger (ACT) traces were recorded simultaneously for all subjects at both field strengths (Fig.1). End-expiratory breath-hold short axis views of the left ventricle were acquired using 2D CINE SSFP (FOV=(320x320) mm^2, matrix size=192 x 192, 25 cardiac phases, 13 slices, slice thickness=8 mm, 1.5 T: α = 60°, TR = 3.3 ms, TE = 1.7 ms; 3.0 T: α = 37°, TR = 2.9 ms, TE = 1.5 ms). The MR stethoscope consisting of an acoustic sensor and an acoustic wave guide was employed for acoustic signal acquisition and transmission to an external unit. Signal conditioning and conversion were conducted using dedicated electronic circuits, with the ultimate goal of providing a robust waveform immune to interference from EMF. The waveform was delivered to the internal physiological signal controller circuitry of a clinical scanner without modifying the scanner's hardware. For cardiac triggering, the ACT system and the ECG leads were connected to the MR scanner's standard ECG signal input, obviating the need to reposition the patient as shown in Fig 1. LV function parameters were acquired and compared. Endocardial boarder sharpness was determined for ACT and ECG triggered data sets.

Results:

Unlike VCG, ACT provided phonocardiograms at 1.5 T and 3.0 T free of interference from electromagnetic fields or magneto-hydrodynamic effects as demonstrated in Fig. 2 and Fig. 3. In comparison, vector ECG waveforms were susceptible to T-wave elevation and other waveform distortions, which were pronounced at 3.0 T as shown in Fig. 2 and Fig. 3. At 3.0 T the T-wave elevation resulted in its amplitude reaching the same order of magnitude as that of the R-wave as illustrated in (i) Fig. 2 for a single subject over 16 successive cardiac cycles and in (ii) Fig. 3 for all subjects using VCG traces averages over 16 successive cardiac cycles. Left ventricular volumes and ejection fraction deduced from VCG and ACT triggered acquisitions at 1.5 T and 3.0 T are surveyed for each subject in Fig. 4 together with the mean ESV, EDV and EF values across all subjects. As illustrated in Fig. 5, the mean EBS across the entire cardiac cycle derived from VCG triggered 2D CINE SSFP was found to be (1.35±0.11) pixel at 1.5 T and (1.35±0.14) pixel at 3.0 T. In comparison, ACT triggered 2D CINE SSFP yielded a mean endocardial border sharpness of (1.45±0.13) pixel at 1.5 T and (1.31±0.16) pixel at 3.0 T. For both VCG and ACT triggered acquisitions, end-diastolic images showed lower EBS as compared to the EBS observed for cardiac phases of contraction and relaxation as shown in Fig. 5. Fig. 6 shows examples derived from faultless VCG and ACT triggering at 3.0 T. For this slice the mean EBS across the entire cardiac cycle derived from VCG triggered 2D CINE SSFP was found to be (0.92±0.16) pixel at 3.0 T. In comparison, ACT triggered 2D CINE SSFP yielded a mean EBS of (0.96±0.16) pixel at 3.0 T. An example of erroneous VCG triggering is shown in Fig. 7. At 3.0 T this subject's EBS derived from VCG triggered 2D CINE SSFP was (1.33±0.19) pixel. For comparison, ACT triggered 2D CINE SSFP yielded an EBS of (1.06±0.16) pixel.

Discussion and Conclusions:

We have demonstrated the efficacy of ACT for LV function assessment using 2D CINE SSFP. LV function analysis and EBS assessment revealed results with no significant differences for ACT and VCG triggering at 1.5 T and 3.0 T in case of accurate VCG trigger recognition. In contrast, ECG-gated 2D SSFP CINE imaging was prone to cardiac motion artifacts if R-wave mis-registration and mis-synchronisation occurred as indicated by the deterioration in the endocardial border sharpness. In conclusion, ACT's intrinsic insensitivity to interference with electro-magnetic fields renders it suitable for clinical CMR due to its excellent trigger reliability.

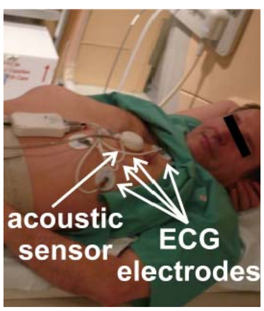

Fig. 1: Clinical setup showing the position of the acoustic sensor and the ECG-electrodes to support simultaneous acquisition of the ECG- and ACT waveform.

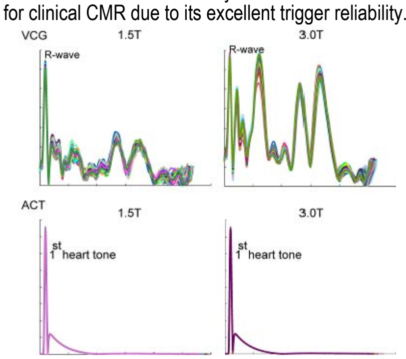

Fig. 2: Traces of the cardiac activity obtained from a single subject over 208 cardiac cycles using acoustic **(bottom)** and ECG **(top)** measurements at 1.5 T **(l)** and 3.0 T **(r)**. Note the T-wave elevation in the ECG due to MHD effects, which are especially pronounced at 3.0 T.

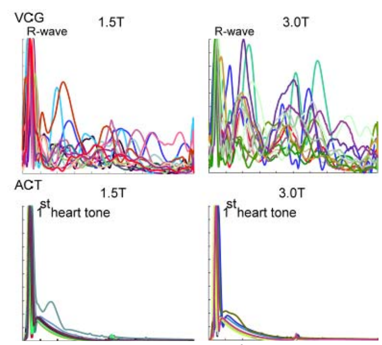

Fig. 3: Normalized mean traces of the cardiac activity obtained for all subjects from acoustic **(bottom)** and electrocardiographic **(top)** measurements at 1.5 T **(l)** and 3.0 T **(r)**. Note the T-wave elevation in the ECG obtained at 3.0 T.

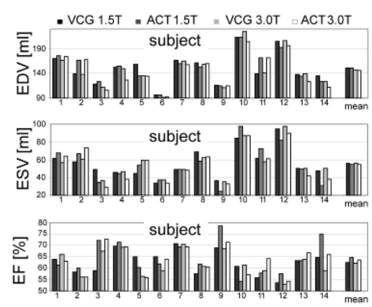

Fig. 4: Left ventricular ESV, EDV and EF measured in 14 healthy subjects at 1.5 T and 3.0 T using VCG and ACT. The mean ESV, EDV, and EF values including data obtained for all subjects are shown on the far right hand side.

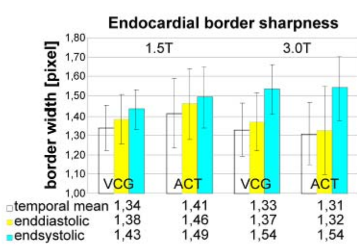

Fig. 5: Enddiastolic, endsystolic and mean endocardial border sharpness (EBS) of 2D SSFP CINE images acquired using vector ECG and MR-stethoscope (ACT) triggering at 1.5 T and 3.0 T.

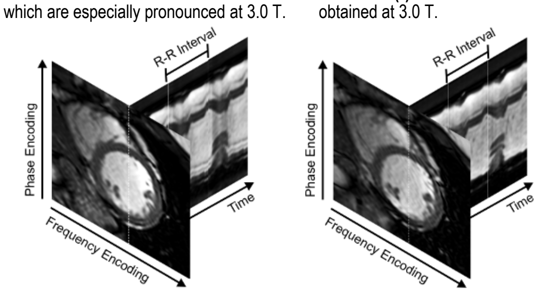

Fig. 6: Short axis views of the heart together with whole R-R interval time series of one-dimensional projections along the profile (dotted line) marked in the short axis view. Data were obtained at 3.0 T using 2D CINE SSFP ACT **(r)** and vector ECG **(l)** cardiac triggering. In this example of correct recognition of the onset of cardiac activity, both ECG and ACT triggered 2D CINE SSFP imaging were found to be immune to the effects of cardiac motion.

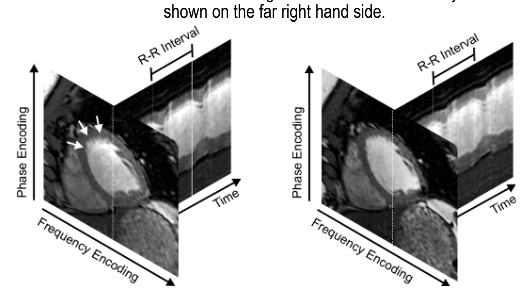

Fig. 7: Short axis views of the heart together with whole R-R interval time series of one-dimensional projections along the profile (dotted line) marked in the short axis view. Data were obtained at 3.0 T using 2D CINE SSFP ACT **(r)** and vector ECG **(l)** cardiac triggering. In this example, ECG-gated 2D SSFP CINE imaging was prone to cardiac motion artifacts (white arrows) caused by R-wave mis-registration due to T-wave elevation. ACT triggered 2D CINE SSFP imaging provided faultless trigger recognition and hence was immune to the effects of cardiac motion.

Reference: 1) Stuber M. et.al., Magn. Reson. Med. 48: 425 (2002); 2) Frauenrath T. et.al., Acta Acustica 94: 148-155 (2008); 3) Frauenrath T, et.al. Inv.radiol. 44:539-547 (2009)